

# Simulation of Switching Arc Using Modified Mayr Arc Model

Member	Yerzan Eshaf	(Toko Electric Corp.)
Member	Masanori Matsuoka	(Toko Electric Corp.)
Non-member	Mitsuhiro Kuramochi	(Toko Electric Corp.)
Non-member	Yoshimasa Taniguchi	(Toko Electric Corp.)
Member	Satoaki Arai	(Tokyo Denki university)

**Abstract:** This paper presents an experimental investigation on interaction between arc voltages and arc length. And a black box arc model based on modified Mayr arc equation is developed to describe the influence of arc length on arc voltages. In this model, the coefficient of arc power loss is defined to be depending on the arc length. The numerical analysis is performed on EMTP. The behavior of arc is represented using Thevenin type-94 component of MODELS.

**Keywords:** switching arc, modified Mayr equation, saw-tooth wave, models type 94 component, EMTP

## 1. Introduction

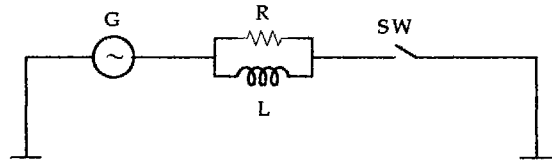
Switching devices are complex elements in electrical power systems. The switching surges in the electrical power systems, that caused by closing or opening operations of switching devices, are generally defined by mutual effects between the arc behavior of switching devices and the corresponding circuit conditions. The aim of a black box arc model is to describe the interaction between the arc and the corresponding circuit. Although a large number of black box arc models based on Mayr's or Cassie's equations have been developed<sup>[1,2,3]</sup>, but contrasting with the models of other elements such as cables or electrical machines, the arc models did not content the increasing demands for the numerical analysis of transient phenomena in electrical power systems, due to the complexity of the physical phenomena of arc.

This paper presents experimental investigation on the arc voltage characteristics of SF<sub>6</sub> gas switches (GS), air switches (AS) and vacuum switches (VS). To describe the influence of arc length on arc voltage, a black box arc model based on modified Mayr arc model is developed. In this model, the coefficient of the arc power loss is modified to be depending on the arc length. The numerical analysis is performed on electromagnetic transients program (EMTP). The behavior of arc is represented using type-94 component of MODELS.

## 2. Characteristics of the arc voltages

The interaction between the arc voltages and arc length in interrupting load currents, using GS, AS and VS is investigated

experimentally. The experimental circuit is shown in Fig. 1. Where GS is a specially designed switch for observing the arc form simultaneously with the arc voltages and the arc currents using a high-speed video camera.



G: generator  
 R and L: load  
 SW: GS, AS and VS

Fig. 1 Experimental circuit

It has been recognized that the arc voltages increase with increase in arc length, and the arc becomes longer due to

- Increase in gap length in separating operation
- Magnetic force of supply current
- Convection of the surrounding gas

### 2.1 Gap length

Fig.2 shows the measured arc voltage and arc current in interrupting load current using GS, AS and VS. In Fig.2 (a), the arc voltage has a tendency to increase with increase in gap length (function of time). The arc voltage  $V_{arc}$  can be divided into two parts of  $V_{oa}$  and  $V_{os}$  as shown in dot lines, where  $V_{oa}$  is the total fall voltage of anode and cathode,  $V_{os}$  is the increase in the arc voltage. For AS as shown in Fig.2 (b), the arc voltage increases with

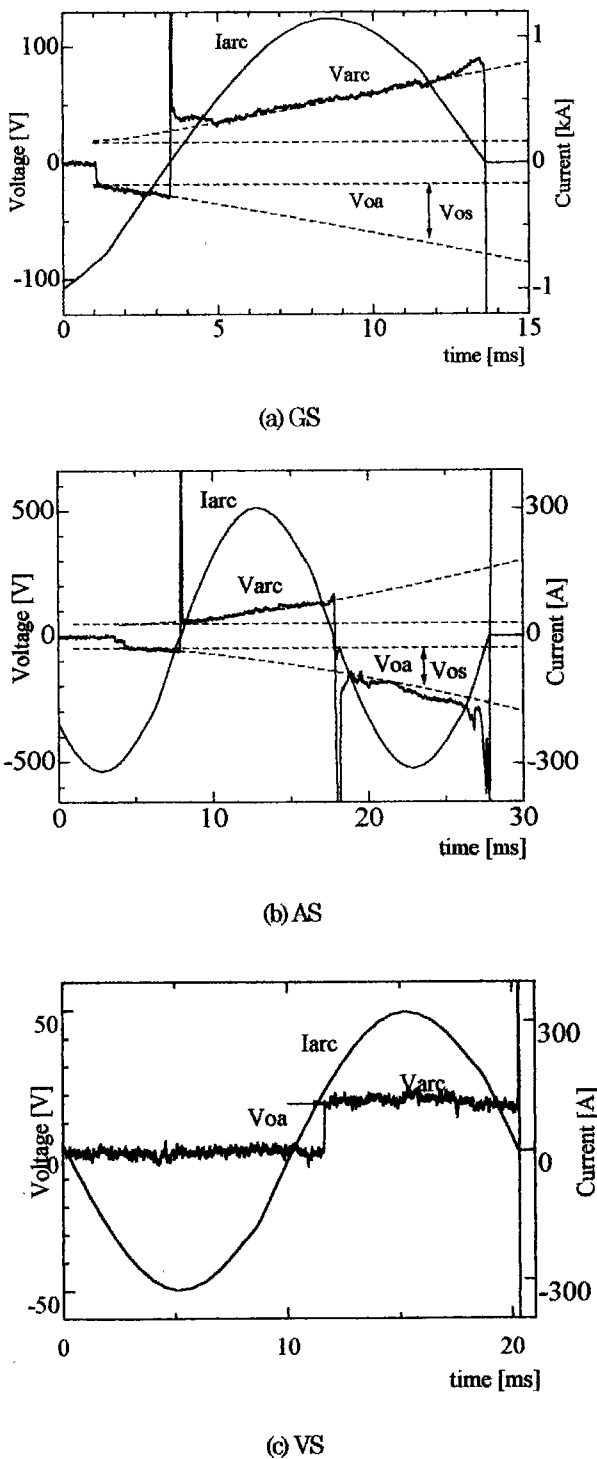


Fig.2 Arc voltage characteristics of GS, AS and VS

increase in gap length as for GS. But there is difference in amplitude of  $V_{oa}$  and  $V_{os}$ , because of the difference in behave of extinction medium as well as separating speed of AS and GS. The arc voltages  $V_{arc}$  of GS and AS can be expressed by Eq.1.  $V_{os}$  can be experimentally expressed by an exponential function of gap length by Eq.2, where  $S$  is gap length, coefficient  $k_s$  and exponent  $\rho$  are constants.

Contrasting with GS and AS, the arc voltage of VS is independent

$$V_{arc} = V_{oa} + V_{os} \quad (1)$$

$$V_{os} = k_s S^\rho \quad (2)$$

of the gap length, and keeps a constant value of  $V_{oa}$  in the whole arcing time, as shown in Fig.2(c). Eq.1 can also be used to represent the arc voltage of VS by omitting  $V_{os}$ .

<2.2> Saw-tooth wave

Fig.3 shows the arc voltage of GS with saw-tooth wave  $V_{ot}$ . In this case, the arc voltage increases with increase in gap length as in Fig.2 (a), and saw-tooth waves  $V_{ot}$ , caused by sharply increases and straightly drops of arc voltages, appeared for several times. The occurrence process of the saw-tooth waves can be explained by the corresponding arc forms that shown in Fig.4, which taken using a high-speed camera simultaneously with the arc voltages and the currents. The axis of contacts is showed by arrows in Fig.4, where the upper is the moving contact and the lower is the state contact. To distinguish the arc path from background, the photographs are processed. Photographs (a)-(d) is the arc profiles around 16, 17, 23 and 24millisec in Fig.3, respectively. The arc paths are nearly in a straight line between two contacts in photograph (a) and (b), and the saw-tooth waves didn't occur during the corresponding time in Fig.3. The arcs are elongated in multiple loops in photographs (c) and (d), and the effective arc length reached up to nearly 5 times as long as in photographs (a) and (b), and the saw-tooth waves appeared during the corresponding time in Fig.3. For the duration before 14millisec in Fig.3 that without saw-tooth waves, the arc forms are similar to those as shown in Fig.4 (a) and Fig.4 (b).

The occurrence of sharply increase of arc voltages is considered due to the magnetic force or the convection of the surrounding gas. And the resin for straightly drop of the arc voltages are considered due to the short circuit of the arc that elongated in multiple-loops.

According to the experimental results, there are statistic characteristics in the occurrence time and the amplitudes of saw-tooth waves. The experiment was carried out for 10 times for each current of 200A, 600A and 800A, respectively. The measured arcing times are within one and half cycle and the saw-tooth wave only occurs in the last half cycle. The incidence of saw-tooth wave increases with increase in arc current, as given in Table.1.

Table.1 Incidence of the saw-tooth

Current (A)	200	600	800
Incidence (%)	0	20	70

The arc voltage with saw-tooth waves can be represented by Eq. 3, where  $V_{ot}$  is a function of time.

$$V_{arc} = V_{oa} + V_{os} + V_{ot} \quad (3)$$

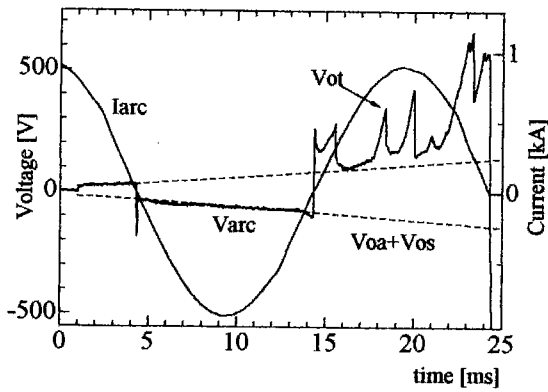


Fig.3 The arc voltage with saw-tooth waves (GS)

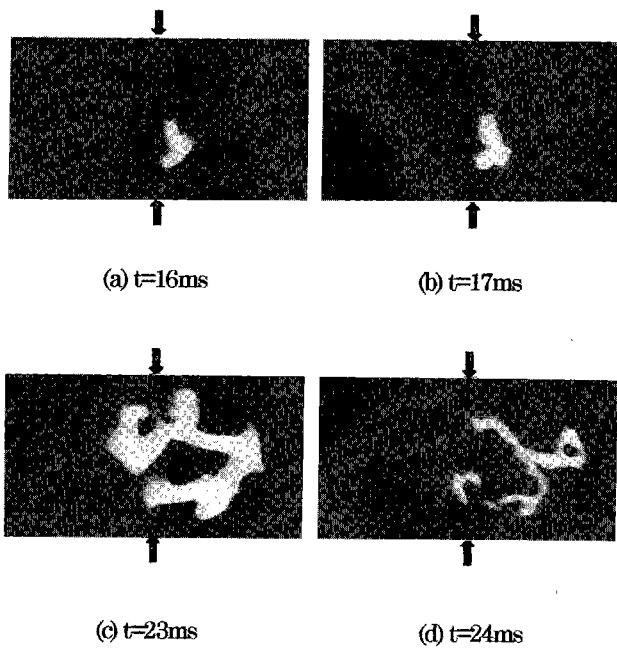


Fig.4 Arc form corresponding to Fig.3

### 3 Numerical analysis

#### 3.1 Arc model

Mayr first described the basic behavior of arc by a black box arc model expressed by Eq. 4,

$$\frac{1}{G} \frac{dG}{dt} = \frac{1}{\theta} \left( \frac{vi}{P} - 1 \right) \quad (4)$$

where  $G$  is arc conductance,  $v$  and  $i$  are arc voltage and arc current, respectively. Since the time constant  $\theta$  and power loss  $P$  are constant, this model was only used to describe the arc behavior qualitatively, but it cannot be used for quantitative analysis. Along with the progress in techniques of the experimental measurement and the numerical simulation, a great number of modified arc models with variable parameters or combinations of several models were proposed.

T.E.Browne<sup>[3]</sup> and Grega Bizjak<sup>[8]</sup> described the arc by a combined Cassie-Mayr equation. Where using Cassie model before current zero, and Mayr model after current zero, and constant arc parameters  $\theta$  and  $P$  were used.

E.V.Bonin<sup>[9]</sup> proposed an arc model which expressed by Eq.5, on the assumption that the arc time constant  $\theta$  and the arc power loss  $P$  of the original Mayr model Eq.4 depended on the arc conductance  $G$ . Eq.5 is generally called as modified Mayr arc model. This model is very sensitive in current zero period and useful for simulation of high-frequency extinction of GCB<sup>[4]</sup>.

$$\frac{1}{G} \frac{dG}{dt} = \frac{1}{\theta_0 G^\alpha} \left( \frac{vi}{P_0 G^\beta} - 1 \right) \quad (5)$$

These models described above are insufficient for calculating the arc voltage characteristics described above in their original formula, because the arc voltage at the peak value of arc current will be the same value of  $V_{oa}$ . This can be proved by Fig. 5 where the arc voltages at the peak values of arc current, calculated by using Eq. 5 with a constant value of  $P_0$ , are equal to  $V_{oa}$ , shown by dot line.

Recently, M.Kizikay<sup>[5]</sup> presented an arc model based on the equation of Hochrainer to calculate the fault arc in air. Where the stationary arc voltage was assumed to be not constant for fault arcs burning in air freely, but it depends on the arc length and partly on the short-circuit current flowing through the arc. The influence of the arc length on the arc voltages for secondary arcs was expressed by defining the stationary arc voltage or the arc time constant as a function of arc length.

In this paper, the modified Mayr arc model Eq.5 is used to describe the dynamic behavior of switching arc. To represent the rise of arc voltage with increase in arc length described above, we assumed that the arc power loss  $P$  to be depending on the arc length. According to Eq. 3, the coefficient  $P_0$  is divided into three parts as expressed in Eq. 6,

$$P_0 = P_{oa} + P_{os} + P_{ot} \quad (6)$$

where,  $P_{oa}$ ,  $P_{os}$  and  $P_{ot}$  are assumed to be corresponding to  $V_{oa}$ ,  $V_{os}$  and  $V_{ot}$  in Eq. 3, respectively.  $P_{oa}$  is a constant, and Eq. 6 becomes the coefficient of Eq. 5 when  $P_{os}$  and  $P_{ot}$  are omitted. To express the effects of the gap length on the arc voltages represented by Eq.2,  $P_{os}$  is determined as a function of gap length as,

$$P_{os} = K_p S^\sigma \quad (7)$$

where  $k_p$  and  $\sigma$  are constant,  $S$  is gap length. The third component  $P_{ot}$ , which applied to represent the saw-tooth waves  $V_{ot}$ , is represented by Eq. 8,

$$P_{ot} = \lambda \left( e^{(t-t_n)^j} - 1 \right) \sum_{n=1}^n (u(t-t_n) - u(t-t_n-\Delta T)) \quad (8)$$

where  $u(t)$  is a unit step function,  $t_n$ ,  $\Delta T$  and  $n$  are the occurrence

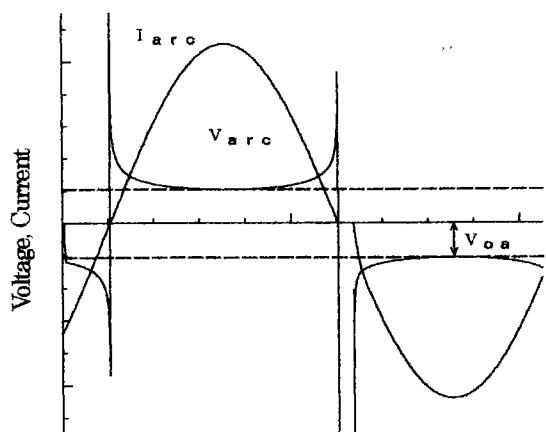
time, the width and the occurrence numbers of saw-tooth waves, respectively.  $\lambda$  and  $\gamma$  are constants. As an example, Fig. 5 (b) shows the calculated arc voltages and currents by using Eq. 5, where  $P_0$  is described by Eq. 6 ( $P_{ot}=0$ ). Compared with the calculation result of using a constant value for  $P_0$  shown in Fig. 5(a), Fig. 5(b) is corresponding to the measured characteristics of arc voltage shown in Fig.2 well.

The arc parameters of Eq.5 can be derived from the measured waveforms of arc voltages and arc currents, but in this paper, it is difficult to derive the arc parameters precisely, due to the influence of  $V_{os}$  and  $V_{ot}$ . In this paper, the same values of  $\alpha=0.5$ ,  $\beta=1.0$  are applied to three type switches. For  $\theta_0$ , the maximum values for which the successful arc extinction occurred is applied. For the other parameters, the value that suitable for the measured waveforms are applied. The initial condition of arc conductance is 0.2S, and the limit value of arc conductance for extinction is  $10^{-10}$ S.

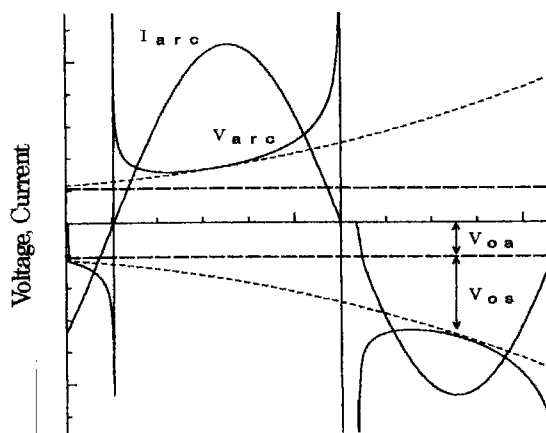
Although it has been pointed out that Eq. 5 was only applicable to air and  $SF_6$  gas arcs, it was unsuited to vacuum arcs because the

thermal process is less significant in vacuum switch devices. We have proved that as a mathematical model, Eq. 5 was applicable to calculate the arc voltages and arc currents of vacuum switch<sup>[8]</sup>.

The numerical calculation is performed on EMTP, and the arc equation is calculated using nonlinear component TYPE94 of MODELS.

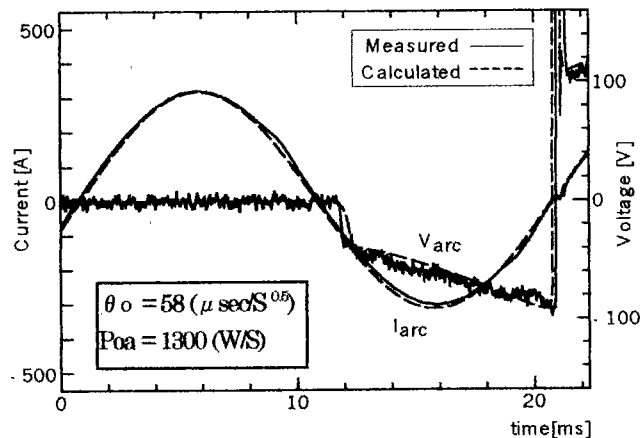


(a)  $P_0=Constant$

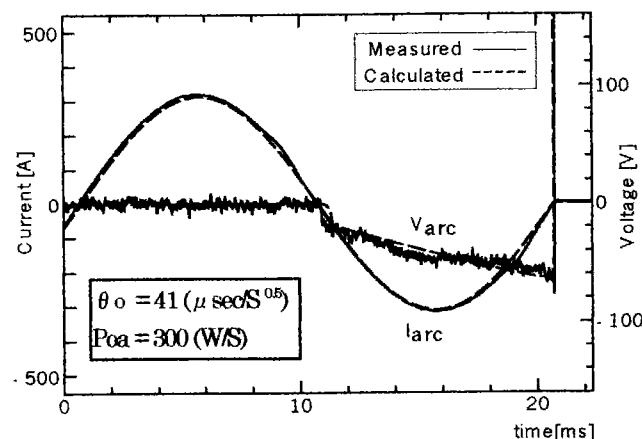


(b)  $P_0=P_{oa}+P_{os}$

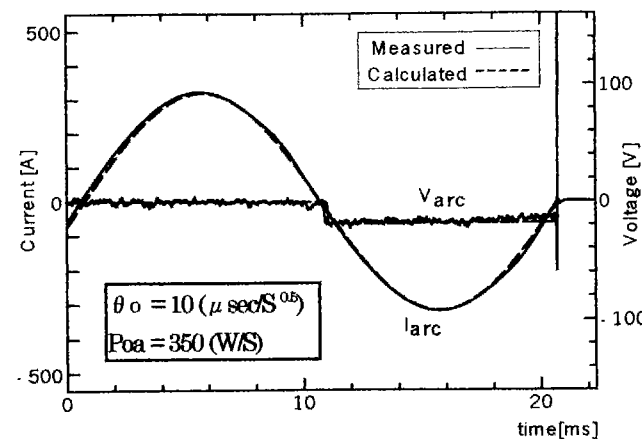
Fig.5 Calculated arc voltage and current



(a) AS



(b) GS

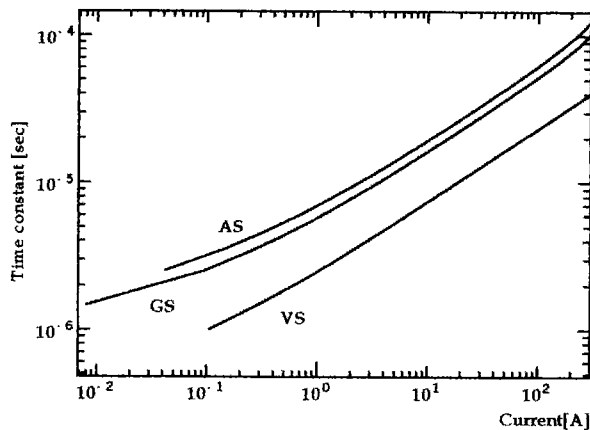


(c) VS

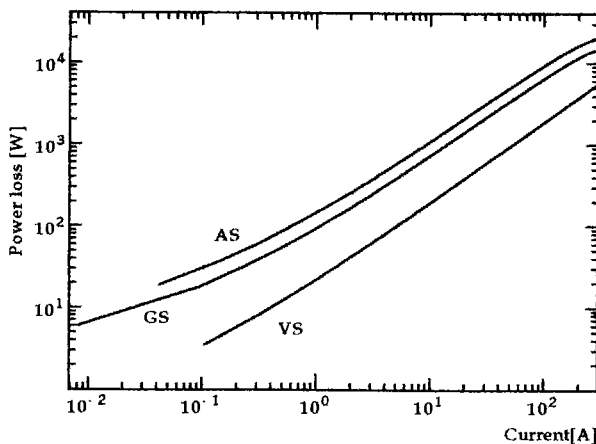
Fig.6 Extinction behavior of AS, GS and VS

### 3.2 Calculated results

3.2.1 Extinction behavior Fig. 6 shows the difference in the extinction behavior of AS, GS and VS. For all cases, the arc current is 200A and the arcing time is half cycle. The successful arc extinction occurred in the case of using GS and VS, but reignition occurred in the case of using AS. The variation of the arc time constant  $\theta$  and the arc power loss  $P$  against to the arc currents are shown in Fig.7. Both  $\theta$  and  $P$  decrease in the order of AS, GS and VS. The calculated values of  $\theta$  for air was larger than that for  $SF_6$ <sup>[7]</sup>, but the value of  $\theta$  and  $P$  for AS and GS is very similar in this paper. Although the conditions such as extinguishing chamber and extinguishing method for AS, GS and VS are different in this paper, but the main reason for that is that the AS used in this paper has an arc extinction pipe, and arc extinction effect is mainly based on the cracked gas from the arc extinction pipe.



(a) Arc time constant vs arc current



(b) Arc power loss vs arc current

Fig. 7 Arc time constant and power loss

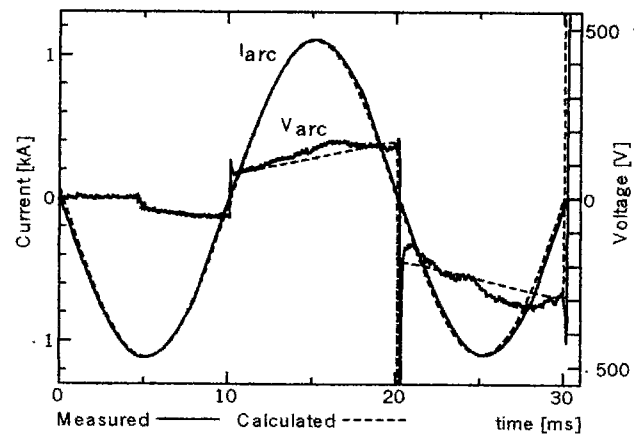
### 3.2.2 Influence of gap length

Fig.8 shows the measured and calculated results of arc voltage of AS. In this case, reignition occurred for two times in current zero, where, the measured dielectric voltages in the current zero were used in calculation. Good agreement between the calculated and

the measured results of the arc voltage was achieved. Same result is obtained for GS.

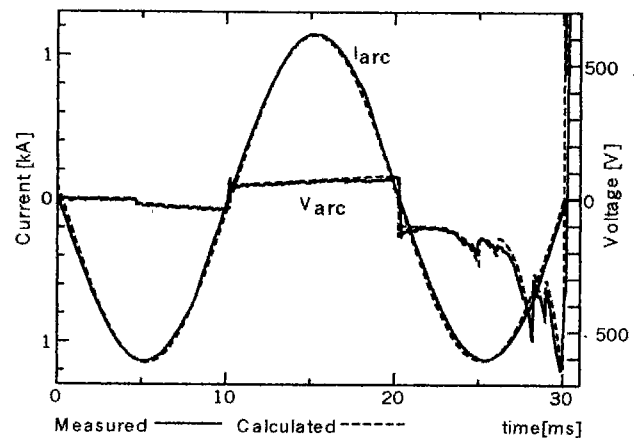
### 3.2.3 Saw-tooth waves

Fig.9 shows the measured and calculated results of arc voltage of GS with the saw-tooth wave. The quantitative calculation for all cases is difficult, because of the statistic characteristics in the occurrence time and the amplitude of the saw-tooth wave.



$$\theta_0 = 35 (\mu \text{secS}^{0.5}), P_{oa} = 1300 (\text{W/S})$$

Fig. 8 Influence of gap length on arc voltages (AS)



$$\theta_0 = 25 (\mu \text{secS}^{0.5}), P_{oa} = 300 (\text{W/S})$$

Fig. 9 Saw-tooth wave

## 4. Conclusions

This paper presented an experimental investigation on the characteristics of arc voltages, and a black box arc model based on modified Mayr arc model was developed to describe the influence of the arc length on the arc voltages. In this model, it was assumed that the coefficient of arc power loss  $P_0$  to be consisted of three components of  $P_{oa}$ ,  $P_{os}$  and  $P_{ot}$ , according to the characteristics of

measured arc voltage. Although the derivation of the parameters relevant to the model and the representation of the statistic characteristics of saw-tooth wave are difficult. But the simulation method is considered to be applicable to various types of switches such as GS, AS and VS, by choosing suitable parameters for each type of switch. It is the subject to investigate the statistic characteristics of saw-tooth wave.

(Manuscript received December 28, 2000, revised July 16, 2001)

#### References

- [1] T. E. Browne, "Practical modeling of the circuit breaker arc as a short line fault interrupter", IEEE Transaction on Power Apparatus and system, Vol. PAS-97, No.3, May/June 1978.
- [2] Grega Bizjak, Peter Zunko, Dusan Povh, "Circuit breaker model for digital simulation based on Mary's and Cassia's differential arc equation", IEEE Transaction on Power Delivery, Vol. 10, No.3, July 1995.
- [3] E. V. Bonin, et al "Advanced Methods of Circuit-Breaker Engineering", Conf. on High Voltage Switching Equipment, Sydney (May 29-30, 1979)
- [4] E.zaima, S.Okabe, S.Nishiwaki, M.Ishikawa, K.Suzuki, H.Tbda, "Application of dynamic arc equations to high-frequency arc extinction in SF<sub>6</sub> gas circuit breakers", IEEE Transaction on Power Delivery, Vol. 8, No.3, July 1993
- [5] M.Kizilcay, "Evaluation of existing secondary arc models", EEUG News May 1997.
- [6] Y. Eshaf, S. Hamada, S.Arai, "Calculation of high-frequency current interruption in vacuum switch", T.IEE Japan, Vol. 117-B, No.12, 1997.
- [7] Y.Yokomizu, K.Ito, T.Kojima, T.Matsumura, "Time constants and conductance of wall-stabilized arcs burning in different gases", IWHV2000, ED-00=121, SP-00-29, HV-00-39, November, 2000.

Yerzan Eshaf (Member) was born on Oct. 3, 1964. He received the M.S. and Ph.D. degrees in electrical engineering from Tokyo Denki University in 1996 and 1999, respectively. He joined Ttko Electric Corporation in 1999. His research interests include the simulation of the arc and the transient phenomena in electrical circuits.



Masanori Matsuoka (member) received the Ph.D. degree in electrical engineering from Tokyo Denki University in 1999. Presently, he is a General Manager of Engineering R&D Development Laboratory of Ttko Electric Corporation. He has worked on development of devices and systems for the distribution systems.



Mitsuhiro Kurimoto (non-member) was born on Apr. 3, 1967. He graduated from the electric course of Nippon Engineering College in 1990. He joined Ttko Electric Corporation in 1999. His research interests include the high voltage testing technology, arc discharge and the analysis of the switching surges.



Yoshimasa Taniguchi (non-member) was born on Apr. 11, 1968. He received the B. S. degree in mechanical engineering from Chiba Industrial University in 1992. He joined Ttko Electric Corporation in 1992. His research interests include the design and development of switchgear.



Satoaki Arai (member) received the Ph.D. degree in electrical engineering from Tokyo Denki University in 1968. Presently, He is a professor at Tokyo Denki University. He is currently interested in the current limiting fuses, electromagnetic transient and arc phenomena.

